



# Simultaneous extraction of multiple orientational constraints of membrane proteins by $^{13}\text{C}$ -detected N–H dipolar couplings under magic angle spinning

Sarah D. Cady, Mei Hong\*

*Department of Chemistry, Iowa State University, Ames, IA 50011, USA*

Received 16 October 2007; revised 2 January 2008

## Abstract

A  $^{13}\text{C}$ -detected N–H dipolar coupling technique is introduced for uniaxially mobile membrane proteins for orientation determination using unoriented samples. For proteins undergoing rigid-body uniaxial rotation in the lipid bilayer, the intrinsic equality between the dipolar coupling constants measured in unoriented samples and the anisotropic coupling measured in static oriented samples has been shown recently. Here, we demonstrate that the orientation-sensitive backbone N–H dipolar couplings can be measured with  $^{13}\text{C}$  detection using 2D and 3D MAS correlation experiments, so that maximal site resolution can be achieved and multiple orientational constraints can be extracted from each experiment. We demonstrate this technique on the M2 transmembrane peptide of the influenza A virus, where the N–H dipolar couplings of various residues fit to a dipolar wave for a helical tilt angle of  $37^\circ$ , in excellent agreement with data obtained from singly  $^{15}\text{N}$ -labeled samples.

© 2008 Published by Elsevier Inc.

*Keywords:* Membrane proteins; Helix orientation; MAS; N–H dipolar coupling; Dipolar wave; Solid-state NMR; Uniaxial motion

## 1. Introduction

Orientation determination of membrane proteins by solid-state NMR traditionally requires mechanically or magnetically aligned proteins under the static condition [1,2]. The alignment results in resolved spectra with anisotropic frequencies—chemical shift or dipolar coupling—indicative of the protein orientation relative to the membrane normal. While this approach has been successfully used to determine the orientation of many membrane peptides and proteins [1,3], macroscopic alignment is a rate-limiting step to this technique. High-quality alignment usually requires extensive optimization of sample conditions such as the types of lipids, the protein/lipid molar ratio, and the degree of hydration. These factors can severely restrict the determination of membrane protein

orientation. To facilitate membrane protein orientation determination, we have recently introduced a powder sample approach that relies on the presence of uniaxial rotational diffusion of the protein in the lipid bilayer [4,5]. When the protein undergoes rigid-body uniaxial rotation with respect to the bilayer normal, the NMR order parameters depend on the angle between the molecule-fixed spin interaction tensor and the motional axis. Thus, by measuring the motionally averaged dipolar couplings or chemical shift anisotropies in powder samples, one can extract the same orientation information as in aligned samples.

We previously demonstrated this powder-sample orientation determination technique on a tetrameric  $\alpha$ -helical bundle, the M2 transmembrane domain (M2TMP) of the influenza A virus, by measuring, on singly  $^{15}\text{N}$ -labeled samples, the static  $^{15}\text{N}$  chemical shift powder patterns and the N–H dipolar couplings under magic-angle spinning (MAS) using the DIPSHIFT [6] method [4]. The choice of  $^{15}\text{N}$  spin interactions is natural because their principal axis systems

\* Corresponding author. Fax: +1 515 294 0105.  
E-mail address: [mhong@iastate.edu](mailto:mhong@iastate.edu) (M. Hong).

are approximately along the helix axis, thus their spectra are sensitive to the tilt and rotation angles of the helical axis. However, to obtain many orientational constraints simultaneously, static chemical shift anisotropy (CSA) measurement with no site resolution is clearly undesirable. Even if MAS-based 2D  $^{15}\text{N}$  CSA or N–H dipolar recoupling techniques are used to give site-resolved information, the  $^{15}\text{N}$  isotropic shift resolution is usually limited compared to the  $^{13}\text{C}$  spectra. The chemical shift ranges for  $\alpha$ -helical proteins, defined as twice the standard deviations, are about 6.0 ppm for  $^{15}\text{N}$  and 8.5 ppm for  $^{13}\text{C}\alpha$  [7]. Considering that the typical  $^{13}\text{C}$  linewidths of membrane proteins are 1–2 ppm whereas the  $^{15}\text{N}$  linewidths are often about 3 ppm, the effective resolution, estimated as the shift range/linewidth ratio, is 2–4 times higher for  $^{13}\text{C}\alpha$  than  $^{15}\text{N}$ . Moreover,  $^{13}\text{C}$  detection has higher sensitivity than  $^{15}\text{N}$ . Thus, it is desirable to convert the  $^{15}\text{N}$ -detected N–H dipolar coupling experiment to  $^{13}\text{C}$  detection. Further, it would be desirable to use two chemical shift dimensions instead of one to resolve the resonances and using a third dimension to sample the N–H dipolar evolution. The challenge is to carry out the necessary coherence transfer between  $^{13}\text{C}$  and  $^{15}\text{N}$  nuclei under the condition that the protein is mobile, which entails reduced dipolar couplings and possibly unfavorable relaxation properties. Provided that this coherence transfer is feasible, the N–H dipolar couplings from multiple residues can be measured simultaneously with  $^{13}\text{C}$  detection to map out the orientation of the protein. It is not essential to measure the  $^{15}\text{N}$  chemical shift anisotropies since the N–H dipolar couplings exhibit a periodicity with respect to residue number that is already sufficient for determining the helix orientation. The residue-periodic N–H dipolar couplings yield the so-called dipolar wave [8], which contains full information on the tilt and rotation angles of the protein. In this work, we show that such a  $^{13}\text{C}$ -detected N–H dipolar wave method is indeed feasible under MAS for an unoriented membrane protein with the requisite uniaxial mobility.

## 2. Materials and methods

Uniformly  $^{13}\text{C}$ ,  $^{15}\text{N}$ -labeled and Fmoc-protected amino acids were either obtained from Sigma (Miamisburg, OH) and Cambridge Isotope Laboratories (Andover, MA), or prepared in house. The transmembrane domain of the M2 protein of the Udorn strain of influenza A virus [9] was synthesized by PrimmBiotech (Cambridge, MA) and purified to >95% purity. The amino acid sequence is SSDPLVVAASIIGILHLILWILDRL. Two peptide samples each containing four U- $^{13}\text{C}$ ,  $^{15}\text{N}$ -labeled residues were synthesized. The first sample contains  $^{13}\text{C}$ ,  $^{15}\text{N}$ -labeled residues at L26, A29, G34 and I35. The second sample contains labels at V27, A30, I33 and L38.

M2TMP was reconstituted into liposomes by a detergent dialysis protocol [10]. Briefly, 1,2-dilauroyl-*sn*-glycero-3-phosphatidylcholine (DLPC) (Avanti Polar Lipids)

was suspended in 1 mL phosphate buffer (10 mM  $\text{Na}_2\text{HPO}_4/\text{NaH}_2\text{PO}_4$ , 1 mM EDTA, 0.1 mM  $\text{NaN}_3$ , 10 mM amantadine) at pH 7.5. 10 mM amantadine is present in all solutions. The lipid solution was vortexed and freeze-thawed to make uniform vesicles of about 200 nm in diameter. M2TMP was codissolved with the detergent octyl- $\beta$ -D-glucopyranoside (OG) in 2 mL phosphate buffer at an OG concentration of 30 mg/mL. The M2TMP/OG solution was then mixed with the DLPC vesicle solution, reaching an OG concentration of 15 mg/mL. The mixture was vortexed for 1 h, allowed to stand for 6–8 h at room temperature, and dialyzed against 1 L phosphate buffer at 4 °C while changing the buffer every 8–12 h for 3 days. The dialyzed M2TMP/DLPC solution was centrifuged at 150,000g for 3 h at 10 °C to give a membrane pellet that is about 50 wt% hydrated. The final protein/lipid molar ratio is 1:15. UV-VIS absorption and photometric assay of the supernatant showed 98% binding of the peptide to the membrane.

Solid-state NMR experiments were carried out on a Bruker AVANCE-600 (14.1 Tesla) spectrometer using a 4 mm triple-resonance MAS probe. Typical 90° pulse lengths for  $^1\text{H}$ ,  $^{13}\text{C}$  and  $^{15}\text{N}$  were 4, 5 and 6  $\mu\text{s}$ , respectively.  $^1\text{H}$  decoupling strengths were 71 kHz during  $^{13}\text{C}$ – $^{15}\text{N}$  REDOR and acquisition, and 76.5 kHz FSLG homonuclear decoupling during N–H dipolar dephasing.

N–H dipolar waves for various orientations were calculated using a home-written Fortran program. A 25-residue ideal  $\alpha$ -helix is used as the input structure for the calculation and is rotated to different tilt angles with respect to the  $z$ -axis. The calculated N–H dipolar couplings are plotted against the residue number and fit to a sinusoidal equation  $y(\tau, \rho) = C(\tau) + A(\tau) \sin((2n \cdot \frac{100}{360} + \phi(\rho))\pi)$ , where the offset  $C(\tau)$  and amplitude  $A(\tau)$  reflect the tilt angle while the phase  $\phi(\rho)$  of the wave depends on the rotation angle  $\rho$ . The rotation angle in the simulation was fixed to within 10° by our previous orientation data obtained in DLPC bilayers [4,11] and the data of Cross and coworkers measured in DMPC bilayers [12]. It was subsequently held constant in the simulations. This is reasonable because the proton channel function of the M2TMP helical bundle dictates that the helices have a well defined rotation angle that places certain residues in the channel lumen to carry out the proton conduction and gating functions [13].

## 3. Results and discussion

### 3.1. Pulse sequence

Fig. 1 shows the  $^{13}\text{C}$ -detected N–H dipolar coupling pulse sequences in the 2D or 3D mode.  $^{13}\text{C}$ – $^{15}\text{N}$  two-spin coherences are generated from  $^{13}\text{C}$  magnetization by a REDOR pulse train [14]. The resulting  $^{15}\text{N}$  antiphase magnetization is allowed to evolve under the scaled N–H dipolar coupling for a period  $t_1$ . Subsequently,  $^{15}\text{N}$  chemical shift evolution may be added as the  $t_2$  dimension if the 3D experiment is desired. The  $^{15}\text{N}$  antiphase magnetization

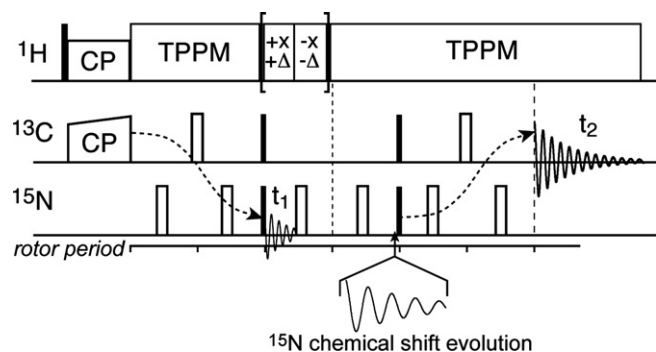


Fig. 1. Pulse sequence for the  $^{13}\text{C}$ -detected N–H dipolar coupling measurement. The  $^1\text{H}$  homonuclear decoupling sequence depicted is FSLG. The optional  $^{15}\text{N}$  chemical shift evolution period can be inserted to make this a 3D experiment to enhance site resolution.

is then reconverted back to  $^{13}\text{C}$  magnetization using an identical REDOR pulse train, and detected in the  $t_3$  period. Thus, the  $^{13}\text{C}$  and  $^{15}\text{N}$  coherence transfer is achieved in an out-and-back heteronuclear single-quantum coherence fashion [15].

During the N–H dipolar evolution period, frequency-switched Lee-Goldburg (FSLG)  $^1\text{H}$  homonuclear decoupling [17] was applied for a whole rotor period, while a  $^{15}\text{N}$   $180^\circ$  pulse was moved through the rotor period to induce dipolar dephasing. A second rotor period with  $^1\text{H}$  heteronuclear decoupling and a synchronously moving  $^{15}\text{N}$   $180^\circ$  pulse refocuses the chemical shift anisotropy encoded in the first rotor period while retaining the N–H dipolar phase. As shown before, this method doubles the dipolar dephasing compared to the case of incrementing the  $^1\text{H}$  homonuclear decoupling period [18]. Due to the short cycle time of the FSLG sequence, relatively fast spinning speeds of 7–10 kHz can be used, which is necessary for suppressing residual  $^{13}\text{C}$ – $^{13}\text{C}$  dipolar interactions in uniformly  $^{13}\text{C}$  labeled proteins.

### 3.2. Model peptide formyl-MLF

We first demonstrate this  $^{13}\text{C}$ -detected N–H dipolar coupling experiment on U- $^{13}\text{C}$ ,  $^{15}\text{N}$ -labeled formyl-MLF, a rigid crystalline peptide with good spectral resolution [19,20]. Fig. 2 shows the  $^{15}\text{N}$  1D CP-MAS spectrum and the  $^{13}\text{C}$  spectrum after passing through the  $^{13}\text{C}$ – $^{15}\text{N}$  REDOR filter. For this well ordered crystalline peptide, the  $^{15}\text{N}$  spectrum is already resolved for the three sites; however this is not generally true for membrane proteins. Fig. 2c and d show the 2D  $^{13}\text{C}$ – $^{15}\text{N}$  correlation spectra with no N–H dipolar evolution (c) and with half a rotor period of dipolar evolution (d), measured using the 3D mode of the pulse sequence in Fig. 1. Both spectra were plotted with the same absolute-intensity contour levels to show the intensity reduction after  $65\ \mu\text{s}$  of N–H dipolar evolution. At 7 kHz MAS,  $65\ \mu\text{s}$  corresponds to half a rotor period of net evolution. A  $^1\text{H}$  FSLG  $t_{360^\circ}$  pulse length of  $13.06\ \mu\text{s}$  was used in the experiment.

The N–H dipolar dephasing curves of the three residues are plotted in Fig. 3. The data of three experiments are shown: the normal 2D  $^{15}\text{N}$ -detected DIPSHIFT curves (triangles), the 2D  $^{13}\text{C}$ -detected DIPSHIFT curves (open squares) using the pulse sequence of Fig. 1 without  $^{15}\text{N}$  chemical shift evolution, and the 3D  $^{13}\text{C}$ – $^{15}\text{N}$  resolved DIPSHIFT curves (filled squares). All three methods produced the same couplings of 11.7 kHz for each residue within experimental uncertainty, which is  $\pm 0.5$  kHz or smaller. The  $^{13}\text{C}$ -detected spectra were obtained using a  $^{13}\text{C}$ – $^{15}\text{N}$  REDOR mixing time of 1.42 ms, including the excitation and reconversion periods. When shorter  $^{13}\text{C}$ – $^{15}\text{N}$  mixing times were used, we found that the  $^{13}\text{C}$ -detected N–H dipolar couplings decreased by  $\sim 10\%$ , indicating incomplete powder averaging that biases the N–H dipolar couplings. With 1.42 ms of  $^{13}\text{C}$ – $^{15}\text{N}$  REDOR coherence transfer, the sensitivity of the experiment on formyl MLF is about 10% of CP. Overall, the consistency between the  $^{13}\text{C}$ -detected and  $^{15}\text{N}$ -detected N–H dipolar dephasing indicates that the technique indeed works as expected.

### 3.3. Influenza A virus M2 transmembrane peptide

For motionally averaged proteins in lipid membranes, the intrinsic sensitivity of the  $^{13}\text{C}$ -detected N–H dipolar coupling experiment is lower due to the small amount of protein in a sample that is largely composed of lipid, and due to the lower efficiency of the  $^{13}\text{C}$ – $^{15}\text{N}$  coherence transfer. Due to motion, the  $^{13}\text{C}$ – $^{15}\text{N}$  dipolar coupling driving the coherence transfer is scaled by the order parameter  $S \equiv \bar{\delta}/\delta = \frac{1}{2}(3\cos^2\theta - 1)$ , where  $\theta$  is the angle between the C–N bond and the motional axis. It is thus necessary to test the feasibility of this technique in a real membrane protein under the condition of uniaxial mobility. We chose the M2 transmembrane protein of the influenza A virus, since its tetrameric helical bundle [21] has been shown to undergo rigid-body uniaxial rotational diffusion around the bilayer normal in DLPC, DMPC and POPC bilayers [4,22]. We carried out the experiment on M2TMP reconstituted in DLPC bilayers with the drug amantadine present [23]. The use of amantadine is essential for the experiment because the drug significantly orders the peptide structure [11], which is manifested by much higher spectral resolution and longer  $^{13}\text{C}$   $T_2$  relaxation times [11]. Without amantadine, the  $\text{C}\alpha$   $T_2$  values are only 1.0–1.8 ms, which makes the efficiency of  $^{13}\text{C}$ – $^{15}\text{N}$  coherence transfer prohibitively low. With amantadine, the  $\text{C}\alpha$   $T_2$  increases to 2.1–3.5 ms [11].

Fig. 4a shows the  $^{15}\text{N}$  CP-MAS spectrum of one of the M2TMP samples. While the linewidth is quite narrow for a membrane protein, two of the sites still overlap completely. The corresponding  $^{13}\text{C}$  spectrum after 1.42 ms of REDOR filter (Fig. 4b), on the other hand, shows complete resolution of the  $\text{C}\alpha$  signals. The use of the  $^{13}\text{C}$ – $^{15}\text{N}$  REDOR filter not only selected the  $\text{C}\alpha$  signals of the protein but also completely removed the lipid background  $^{13}\text{C}$  signals, thus

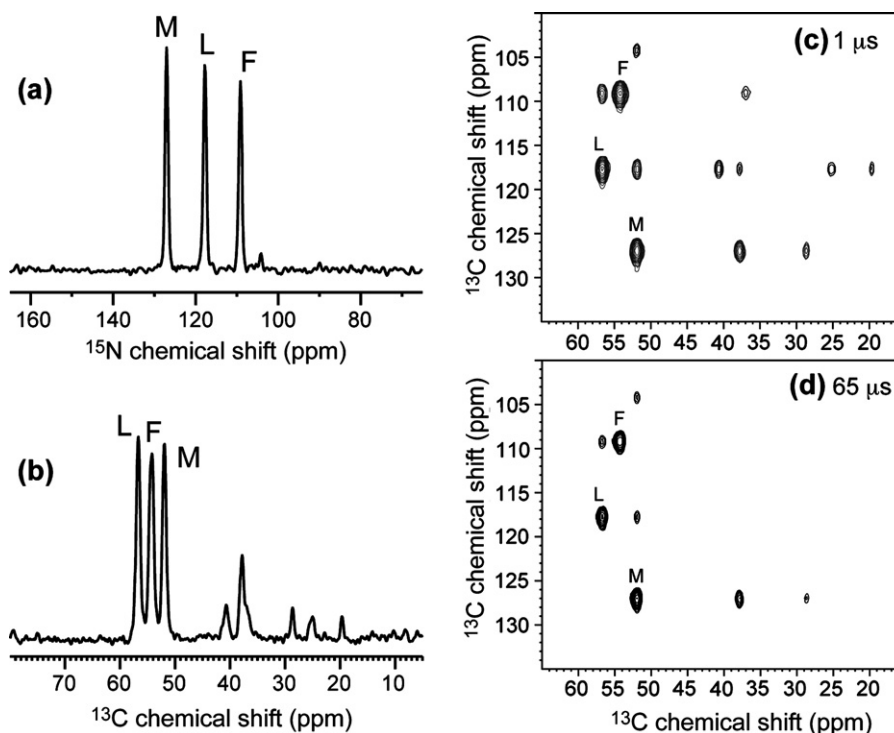


Fig. 2. Detecting N–H dipolar dephasing of formyl-MLF by  $^{13}\text{C}$  detection. (a)  $^{15}\text{N}$  CP-MAS spectrum. (b)  $^{13}\text{C}$  MAS spectrum after a 1.42 ms  $^{13}\text{C}$ – $^{15}\text{N}$  REDOR filter. (c) 2D  $^{13}\text{C}$ – $^{15}\text{N}$  correlation spectrum with no N–H dipolar dephasing. (d) 2D  $^{13}\text{C}$ – $^{15}\text{N}$  correlation spectrum with 65  $\mu\text{s}$  N–H dipolar dephasing. The data were obtained under 7 kHz MAS at ambient temperature.

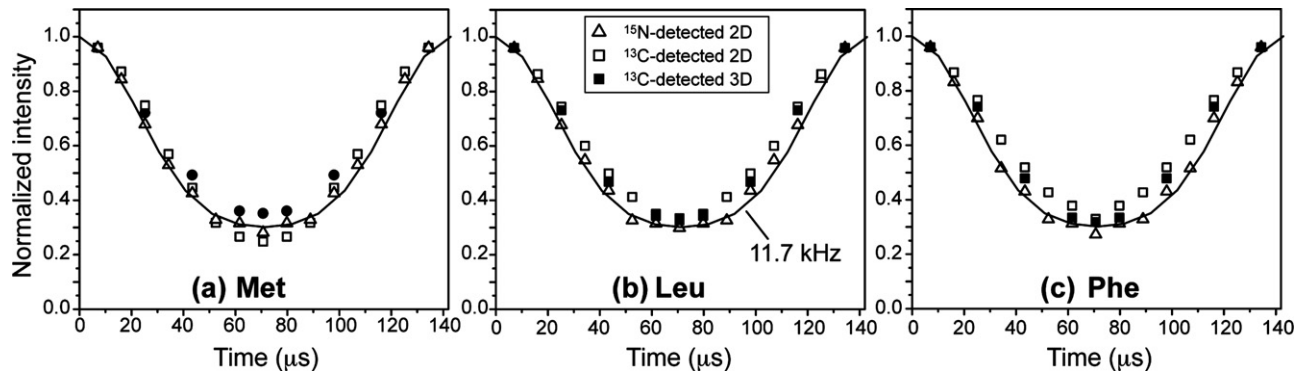


Fig. 3. N–H dipolar dephasing curves of the three residues of formyl-MLF, measured by three methods:  $^{15}\text{N}$ -detected 2D DIPSHIFT (open triangles),  $^{13}\text{C}$ -detected 2D DIPSHIFT (open squares), and  $^{13}\text{C}$ – $^{15}\text{N}$  resolved 3D DIPSHIFT (filled squares).

significantly simplifying spectral assignment. Two representative N–H dipolar dephasing curves, for residues I35 and G34, are shown in Fig. 4(c and d). The curves were measured with  $^{13}\text{C}$  detection without  $^{13}\text{C}$ – $^{15}\text{N}$  correlation. The two residues show very different N–H dipolar couplings of 3.0 and 6.1 kHz, indicating the difference in their N–H bond orientations relative to the motional axis. The two residues have very different sensitivities in the  $^{13}\text{C}$  spectrum; but even the less sensitive G34 signal gave a self-consistent dephasing curve.

A total of six N–H dipolar couplings were resolved and measured in this way. They are plotted with respect to the residue number and shown in Fig. 5. Indeed, the data fit to a periodic pattern, which is best represented by a dipolar

wave for an ideal helix whose axis is tilted by  $37^\circ$  from the bilayer normal. This is in good agreement with the recently measured M2TMP tilt angle in the DLPC bilayer using singly  $^{15}\text{N}$ -labeled samples [4,11].

In Fig. 5, two sites, A30 and L38, exhibit couplings significantly larger than the expected values for the  $37^\circ$  dipolar wave. At present we do not know the exact reason for these outliers. They may partly reflect a true helix axis orientation difference. Cross and coworkers recently reported that the helical segment C-terminal to G34 in M2TMP is kinked from the N-terminal segment in the presence of amantadine [24]. Using glass-plate aligned DMPC membranes, they found a tilt angle of  $30^\circ$  for residues N-terminal to G34 but  $20^\circ$  for residues C-terminal to it. A similar

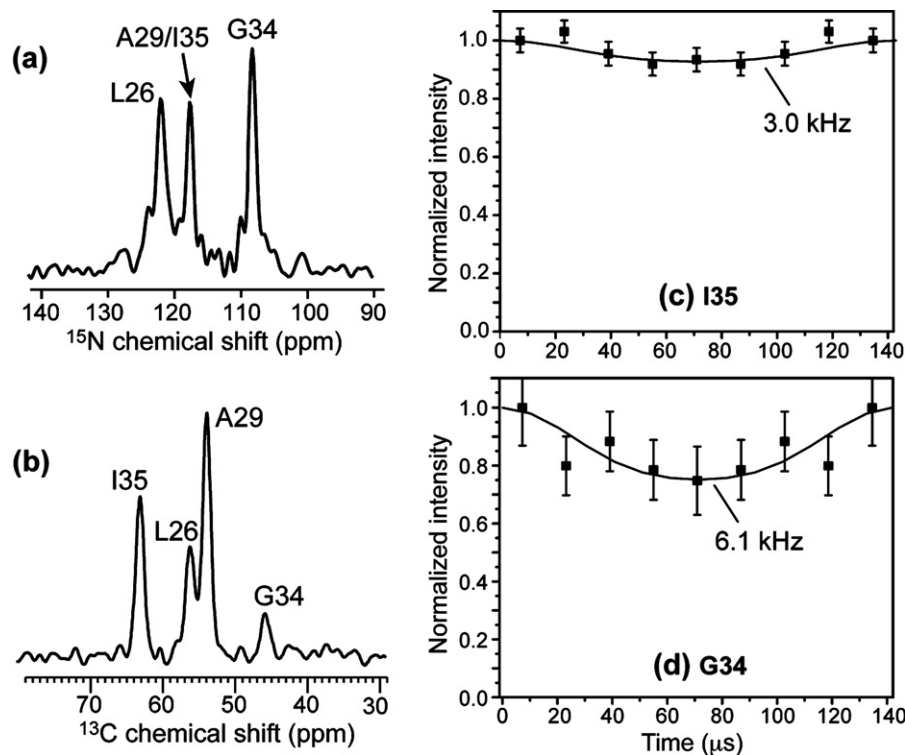


Fig. 4. N–H dipolar couplings of  $^{13}\text{C}$ ,  $^{15}\text{N}$ -labeled amantadine-bound M2TMP in DLPC bilayers at 313 K. (a) 1D  $^{15}\text{N}$  CP-MAS spectrum. Two of the four  $^{15}\text{N}$  labels overlap completely. NS = 5120. (b)  $^{13}\text{C}$  MAS spectrum after 1.42 ms  $^{13}\text{C}$ – $^{15}\text{N}$  REDOR filter. All four  $^{13}\text{C}\alpha$  labels are resolved. NS = 27,648. (c and d)  $^{13}\text{C}$ -detected N–H dipolar dephasing curves for I35 (c) and G34 (d). The couplings indicated are the true values after dividing the fit values by  $1.154 = 0.577 \times 2$  to take into account the FSLG scaling factor 0.577 and the doubling factor of 2. The experiment was conducted under 7 kHz MAS.

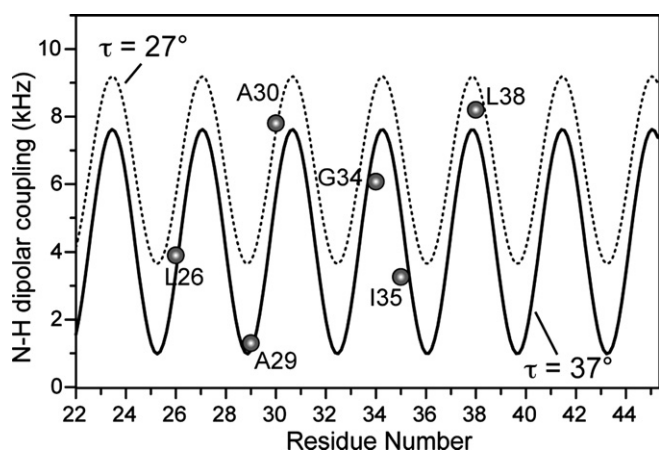


Fig. 5.  $^{13}\text{C}$ -detected N–H dipolar couplings of M2TMP as a function of residue number. The peptide is bound to DLPC bilayers with the drug amantadine present. The calculated wave corresponds to a tilt angle  $\tau$  of  $37^\circ$ . The calculated wave for a tilt angle  $27^\circ$  is also shown for comparison (dotted line).

helix kink may be present in the current DLPC bilayers as well, which could then explain the L38 data. More residues on the C-terminus side of G34 need to be measured to test this hypothesis. Alternatively, the larger couplings could result from deviation of the helix from the ideal backbone conformation. It is certain that the abnormally large couplings do not result from the lack of uniaxial rotation, since the  $^2\text{H}$  spectrum of  $\text{CD}_3$ -labeled A29 in the same sample

showed a quadrupolar coupling of 15.5 kHz (not shown), which is much narrower than the 40 kHz expected when methyl rotation is the only motion. In other words, the peptide backbone must undergo reorientational motion to reduce the  $\text{C}\alpha$ – $\text{C}\beta$  order parameter of A29 to an effective value of 0.39 (relative to the methyl group rigid limit of 40 kHz). We can also rule out segmental motion of A30 and L38 as the reason for the outliers, since any internal motion additional to the whole-body motion can only make the couplings smaller, instead of bigger, than the expected values. Thus, either a true helix orientation change or non-ideal backbone conformation at these residues account for the abnormal N–H couplings.

### 3.4. Sensitivity of the MAS $^{13}\text{C}$ -detected N–H dipolar wave experiment

The  $^{13}\text{C}$ -detected N–H DIPSHIFT data on the amantadine-complexed M2TMP samples required signal-averaging of 23,000–27,000 scans per  $t_1$  slice and nine  $t_1$  slices, thus resulting in a total experimental time of about 5 days per sample. The efficiency of the experiment compared to CP is 5–15%, depending on the  $^{13}\text{C}$   $T_2$  of the individual residues. To increase the sensitivity of the experiment, one could use an alternative method for C–N coherence transfer, which is double cross polarization (CP). The  $^{15}\text{N}$  magnetization can be directly polarized from  $^1\text{H}$  and evolves

under the N–H dipolar coupling. It can then be transferred to  $^{13}\text{C}\alpha$  by frequency-specific CP [16]. Our tests on formyl-MLF showed that indeed this SPECIFIC-CP method has a higher efficiency of  $\sim 40\%$  compared to REDOR at a  $^{15}\text{N}$ – $^{13}\text{C}$  contact time of 3 ms. However, with 3 ms contact, the  $^{13}\text{C}$ -detected N–H dipolar couplings were about 12% weaker than the rigid-limit value (10.4 kHz instead of 11.7 kHz) measured using the direct  $^{15}\text{N}$ -detected DIPSHIFT experiment, suggesting incomplete powder averaging. Increasing the N–C CP contact time to as much as 7 ms did not change the situation. The dephasing value at the middle of the rotor period for Leu was 0.39 for the  $^{13}\text{C}$ -detected DIPSHIFT experiment versus 0.31 for the direct  $^{15}\text{N}$ -detected experiment. For all sites, a 25–50% increase in the intensity in the middle of the rotor period is seen, indicating weaker dipolar couplings. Moreover, using a long C–N contact time places a higher demand on the probe due to the simultaneous radiofrequency irradiation. In real membrane proteins with the requisite mobility, long contact times may also cause potential  $T_{1\rho}$  losses. These shortcomings may be circumvented, however, if the reduced dipolar couplings due to incomplete powder averaging can be calculated and corrected for, in which case this CP-based DIPSHIFT method would be significantly more sensitive.

#### 4. Conclusion

In conclusion, we have demonstrated an MAS  $^{13}\text{C}$ -detected N–H dipolar coupling technique to simultaneously extract multiple orientational constraints of membrane proteins in unoriented lipid bilayers by virtue of their uniaxial motion. The enhanced site resolution provided by  $^{13}\text{C}$  chemical shifts is a significant advantage over the  $^{15}\text{N}$ -detected experiment, and the ability to extend this approach to 3D to further resolve resonances makes this approach more applicable to larger membrane proteins. The elimination of sample alignment and the adoption of MAS technology for orientation determination are major advantages of this approach. In this way, multiple orientation-dependent N–H dipolar couplings can be measured to yield dipolar waves, from which both the helix orientation and helical structure defects can be detected.

For this  $^{13}\text{C}$ -detected  $^{15}\text{N}$ – $^1\text{H}$  dipolar wave technique to be generally applicable, long  $^{13}\text{C}$   $T_2$  is essential to facilitate the  $^{13}\text{C}$ – $^{15}\text{N}$  coherence transfer. In the case of the M2TMP helical bundle, the use of a natural channel blocker, amantadine, made the dynamic property of the protein sufficiently favorable to be amenable to this technique. Future development of more efficient coherence transfer techniques for mobile systems will be desirable to further increase the sensitivity of this class of techniques.

#### Acknowledgment

This work is funded by National Science Foundation Grant MCB-0543473.

#### References

- [1] S.J. Opella, F.M. Marassi, Structure determination of membrane proteins by NMR spectroscopy, *Chem. Rev.* 104 (2004) 3587–3606.
- [2] M. Hong, Oligomeric structure, dynamics, and orientation of membrane proteins from solid-state NMR, *Structure* 14 (2006) 1731–1740.
- [3] R.R. Ketchum, W. Hu, T.A. Cross, High resolution conformation of Gramicidine A in a lipid bilayer by solid-state NMR, *Science* 261 (1993) 1457–1460.
- [4] S.D. Cady, C. Goodman, C.D. Tatko, W.F. DeGrado, M. Hong, Determining the orientation of uniaxially rotating membrane proteins using unoriented samples: a  $^2\text{H}$ ,  $^{13}\text{C}$ , AND  $^{15}\text{N}$  solid-state NMR investigation of the dynamics and orientation of a transmembrane helical bundle, *J. Am. Chem. Soc.* 129 (2007) 5719–5729.
- [5] M. Hong, T. Doherty, Orientation determination of membrane-disruptive proteins using powder samples and rotational diffusion: a simple solid-state NMR approach, *Chem. Phys. Lett.* 432 (2006) 296–300.
- [6] M.G. Munowitz, R.G. Griffin, G. Bodenhausen, T.H. Huang, Two-dimensional rotational spin-echo nuclear magnetic resonance in solids: correlation of chemical shift and dipolar interactions, *J. Am. Chem. Soc.* 103 (1981) 2529–2533.
- [7] H. Zhang, S. Neal, D.S. Wishart, RefDB: a database of uniformly referenced protein chemical shifts, *J. Biomol. NMR* 25 (2003) 173–195.
- [8] M.F. Mesleh, S. Lee, G. Veglia, D.S. Thiriot, F.M. Marassi, S.J. Opella, Dipolar waves map the structure and topology of helices in membrane proteins, *J. Am. Chem. Soc.* 125 (2003) 8928–8935.
- [9] T. Ito, O.T. Gorman, Y. Kawaoka, W.J. Bean, R.G. Webster, Evolutionary analysis of the influenza A virus M gene with comparison of the M1 and M2 proteins, *J. Virol.* 65 (1991) 5491–5498.
- [10] W. Luo, R. Mani, M. Hong, Sidechain conformation and gating of the M2 transmembrane peptide proton channel of influenza A virus from solid-state NMR, *J. Phys. Chem.* 111 (2007) 10825–10832.
- [11] S.D. Cady, M. Hong, Amantadine-induced conformational and dynamical changes of the influenza M2 transmembrane proton channel, *Proc. Natl. Acad. Sci. USA* (2008), in press.
- [12] J. Wang, S. Kim, F. Kovacs, T.A. Cross, Structure of the transmembrane region of the M2 protein H(+) channel, *Protein Sci.* 10 (2001) 2241–2250.
- [13] L.H. Pinto, G.R. Dieckmann, C.S. Gandhi, C.G. Papworth, J. Braman, M.A. Shaughnessy, J.D. Lear, R.A. Lamb, W.F. DeGrado, A functionally defined model for the M2 proton channel of influenza A virus suggests a mechanism for its ion selectivity, *Proc. Natl. Acad. Sci. USA* 94 (1997) 11301–11306.
- [14] T. Gullion, J. Schaefer, Rotational echo double resonance NMR, *J. Magn. Reson.* 81 (1989) 196–200.
- [15] G. Bodenhausen, D.J. Ruben, Natural abundance nitrogen-15 NMR by enhanced heteronuclear spectroscopy, *Chem. Phys. Lett.* 69 (1980) 185–189.
- [16] M. Baldus, A.T. Petkova, J. Herzfeld, R.G. Griffin, Cross polarization in the tilted frame: assignment and spectral simplification in heteronuclear spin systems, *Mol. Phys.* 95 (1998) 1197–1207.
- [17] A. Bielecki, A.C. Kolbert, H.J.M. de Groot, R.G. Griffin, M.H. Levitt, Frequency-switched Lee-Goldburg sequences in solids, *Adv. Magn. Reson.* 14 (1990) 111–124.
- [18] M. Hong, J.D. Gross, C.M. Rienstra, R.G. Griffin, K.K. Kumashiro, K. Schmidt-Rohr, Coupling amplification in 2D MAS NMR and its application to torsion angle determination in peptides, *J. Magn. Reson.* 129 (1997) 85–92.
- [19] C.M. Rienstra, L. Tucker-Kellogg, C.P. Jaroniec, M. Hohwy, B. Reif, M.T. McMahon, B. Tidor, T. Lozano-Perez, R.G. Griffin, De novo determination of peptide structure with solid-state magic-angle spinning NMR spectroscopy, *Proc. Natl. Acad. Sci. USA* 99 (2002) 10260–10265.

- [20] M. Hong, R.G. Griffin, Resonance assignment for solid peptides by dipolar-mediated  $^{13}\text{C}/^{15}\text{N}$  correlation solid-state NMR, *J. Am. Chem. Soc.* 120 (1998) 7113–7114.
- [21] W. Luo, M. Hong, Determination of the oligomeric number and intermolecular distances of membrane protein assemblies by anisotropic  $(1)\text{h}$ -driven spin diffusion NMR spectroscopy, *J. Am. Chem. Soc.* 128 (2006) 7242–7251.
- [22] Z. Song, F.A. Kovacs, J. Wang, J.K. Denny, S.C. Shekar, J.R. Quine, T.A. Cross, Transmembrane domain of M2 protein from influenza A virus studied by solid-state  $^{15}\text{N}$  polarization inversion spin exchange at magic angle NMR, *Biophys. J.* 79 (2000) 767–775.
- [23] C. Wang, K. Takeuchi, L.H. Pinto, R.A. Lamb, Ion channel activity of influenza A virus M2 protein: characterization of the amantadine block, *J. Virol.* 67 (1993) 5585–5594.
- [24] J. Hu, T. Asbury, S. Achuthan, C. Li, R. Bertram, J.R. Quine, F. Riqiang, T.A. Cross, Backbone Structure of the amantadine-block trans-membrane domain M2 proton channel from influenza A virus, *Biophys. J.* 92 (2007) 4335–4343.